processes

MDPI

Article

Model-Based Monitoring of Occupant's Thermal State for Adaptive HVAC Predictive Controlling

Ali Youssef, Nicolás Caballero and Jean-Marie Aerts *

Department of Biosystems, Animal and Human Health Engineering Division, M3-BIORES: Measure, Model & Manage of Bioresponses Laboratory, KU Leuven, Kasteelpark Arenberg 30, 3001 Heverlee, Belgium; ali.youssef@kuleuven.be (A.Y.); nicolas.caballero@gmail.com (N.C.)

* Correspondence: jean-marie.aerts@kuleuven.be

Received: 31 August 2019; Accepted: 5 October 2019; Published: 10 October 2019

Abstract: Conventional indoor climate design and control approaches are based on static thermal comfort/sensation models that view the building occupants as passive recipients of their thermal environment. Recent advances in wearable sensing technologies and their generated streaming data are providing a unique opportunity to understand the user's behaviour and to predict future needs. Estimation of thermal comfort is a challenging task given the subjectivity of human perception; this subjectivity is reflected in the statistical nature of comfort models, as well as the plethora of comfort models available. Additionally, such models are using not-easily or invasively measured variables (e.g., core temperatures and metabolic rate), which are often not practical and undesirable measurements. The main goal of this paper was to develop dynamic model-based monitoring system of the occupant's thermal state and their thermoregulation responses under two different activity levels. In total, 25 participants were subjected to three different environmental temperatures at two different activity levels. The results have shown that a reduced-ordered (second-order) multi-inputs-single-output discrete-time transfer function (MISO-DTF), including three input variables (wearables), namely, aural temperature, heart rate, and average skin heat-flux, is best to estimate the individual's metabolic rate (non-wearable) with a mean absolute percentage error of 8.7%. A general classification model based on a least squares support vector machine (LS-SVM) technique is developed to predict the individual's thermal sensation. For a seven-class classification problem, the results have shown that the overall model accuracy of the developed classifier is 76% with an F1-score value of 84%. The developed LS-SVM classification model for prediction of occupant's thermal sensation can be integrated in the heating, ventilation and air conditioning (HVAC) system to provide an occupant thermal state-based climate controller. In this paper, we introduced an adaptive occupant-based HVAC predictive controller using the developed LS-SVM predictive classification model.

Keywords: thermal sensation; thermal comfort; machine-learning; prediction; adaptive controlling

1. Introduction

Thermal comfort (TC) is an ergonomic aspect determining the satisfaction about the surrounding environment and is defined as "that condition of mind which expresses satisfaction with the thermal environment and is assessed by subjective evaluation" [1]. The effect of thermal environments on occupants might also be assessed in terms of thermal sensation (T_S), which can be defined as "a conscious feeling commonly graded into the categories cold, cool, slightly cool, neutral, slightly warm, warm, and hot" [1]. Thermal sensation and thermal comfort are both subjective judgments, however, thermal sensation is related to the perception of one's thermal state, and thermal comfort to the evaluation of this perception [2]. The assessment of thermal sensation has been regarded as more reliable and. as such. is often used to estimate thermal comfort [3].

Human thermal sensation mainly depends on the human body temperature (core body temperature), which is a function of sets of comfort factors [4,5]. These comfort factors include indoor environmental factors, namely the mean air temperature around the body, relative air velocity around the body, humidity, and the mean radiant temperature to the body [5]. Additionally, some personal (individual-related) factors, namely, metabolic rate or internal heat production in the body, which vary with the activity level and clothing thermal-physical properties (such as clothing insulation and vapour clothing resistance), are included. It should be mentioned that the individual thermal perception is deepening, as well, on psychological factors, including naturalness (an environment where the people tolerate wide changes of the physical environment), expectations and short/long-term experience, which directly affect individuals' perceptions, time of exposure, perceived control and environmental stimulation [6]. The most considered method to have an accurate assessment of T_S is to ask the individuals directly about their thermal sensation perception [4,5]. Thermal sensation mathematical models have been developed in order to overcome the difficulties of direct enquiry of subjects. The development of such models is mostly dependent on statistical approaches that correlates experimental conditions (i.e., environmental and person-related variables) data to thermal sensation votes obtained from human subjects [3,5]. Most of these models (e.g., predicted mean vote, PMV) are static in the sense that they predict the average vote of a large group of people based on the seven-point thermal sensation scale. Instead of individual thermal comfort, they only describe the overall thermal sensation of multiple occupants in a shared thermal environment. To overcome the disadvantages of static models, adaptive thermal comfort models aim to provide insights in increasing opportunities for personal and responsive control, thermal comfort enhancement, energy consumption reduction and climatically responsive and environmentally responsible building design [7,8]. The idea behind adaptive model is that occupants and individuals are no longer regarded as passive recipients of the thermal environment but, rather, play an active role in creating their own thermal preferences [8]. In addition to regression analysis, thermal sensation prediction can also be seen as a classification problem where various classification algorithms can be implemented [7]. Recently, a number of studies (e.g., [9–13]) have demonstrated the possibility of using machine learning techniques, such as a support vector machine (SVM), to assess and predict human thermal sensation. It can be concluded based on the published work (see the recent literature review [7] showing that classification-based models have performed so well as regression models).

Recent advances in mobile technologies in healthcare, in particular wearable technologies (m-health) and smart clothing, have positively contributed to new possibilities in controlling and monitoring health conditions and human wellbeing in daily life applications. The wearable sensing technologies and their generated streaming data are providing a unique opportunity to understand the user's behaviour and to predict future needs [14]. The generated streaming data is unique due to the personal nature of the wearable devices. However, the generated streaming data is forming a challenge pertaining to the need of personalized adaptive models that can handle newly arrived personal data.

Current heating, ventilation, and air conditioning (HVAC) control systems can be divided into two types: air temperature regulator (ATR) and thermal comfort regulator (TCR). Most TCR controllers use static models, mainly PMV, as a performance criterion.

This paper aims to develop an adaptive model for real-time monitoring of human thermal states using personal non-intrusive sensing techniques. The developed model should be suitable for real-time adaptive control of indoor climate systems and smart wearable applications.

2. Materials and Methods

2.1. Experiments and Experimental Setup

2.1.1. Climate Chambers (Body and Mind Room)

The "*Body and Mind Room*" consists of three climate-controlled chambers (A, B and C) designed and built to investigate the dynamic mental and physiological responses of humans to specific indoor

climate conditions. The Body and Mind rooms are experimental facilities at the M3-BIORES laboratory (Animal and Human Health Engineering Division, KU Leuven, Leuven, Belgium). The three rooms are dimensionally identical; however, each room is designed to provide different ranges of climate conditions, as shown in Table 1.

Table 1. The different temperature and relative humidity ranges that can be provided by the different Body and Mind rooms (A, B and C).

Room	Air Temperature Range (°C)	Relative Humidity Range (%)
A	+23–+37	50–80
B	+10–+25	50–80
C	−5–+10	40–60

The three rooms are equipped with axial fans to simulate wind velocities between 2.5 and 50 $km \cdot h^{-1}$.

2.1.2. Experimental Protocol

The experimental protocol used in the present study is designed in such way to investigate the subjects' thermal and physiological responses to predefined three different temperature (*low*, *normal* and *high*) that under two levels of physical activities (seated = *low* and cycling = *high*). The three predefined temperatures (*low* = 5 °C, *normal* = 24 °C and *high* = 37 °C) are chosen based on the thermal comfort chart from [15] and the effects on health according to the Wind Chill Chart for cold exposure (National Weather Service of the US) and for hot temperatures exposure according to [16]. The conducted experiments consist of two phases (Figure 1, upper graph), namely, low activity and high activity phases. During the first experimental phase, low activity phase, the test subjects (while being seated = low activity) are exposed, for 55 min, to three levels of temperatures in the following order: normal, low, high and normal again (Figure 1). During the high activity phase, the test subjects is exposed to a 15 min of light physical stress (80 W of cycling on a fastened racing bicycle). During the course (75 min) of the active phase, each test subject is exposed to the predefined three temperature levels (Figure 1, lower graph). During each temperature level, starting from the normal level (24 °C), the test subjects are performed 15 min of cycling (with 80 W power) and followed 4 min of resting (seated). During the course of conducted experiments, the clothing insulation factor (*Col*) is kept constant at *Col* = 0.34, which accounts for a cotton short and t-shirt as standard clothing for all test subjects. The experimental protocol is approved by the SMEC (Sociaal-Maatschappelijke Ethische Comissie) on 16 January 2019 with number G-2018-12-1464.

2.1.3. Test Subjects

In total, 25 healthy participants (six females and 19 males were asked before the experiments if they had been diagnosed with any cardiac problems, diabetic or any other health problems), between the age of 25 and 35 (average age 26 ± 4.2) years, with average weight and height of 70.90 (±12.70) kg and 1.74 (±0.10) m, respectively, volunteered to perform the aforementioned experimental protocol.

2.1.4. Measurements and Gold Standards

During the course of the experiments, participants' heart rate, metabolic rate, average skin temperature, heat flux between the skin and the ambient air and core body temperature represented by the aural temperature are measured continuously. Heart rate monitoring is performed using a Polar H7 ECG (Polar, Kempele, Finland) strap that is placed under the chest, with a sampling frequency of 128 Hz. The metabolic rate, as metabolic equivalent tasks (METs) of each test subject, is calculated based on indirect calorimetry using a MetaMAX 3B (CORTEX-Medical, Leipzig, Germany) spiroergometer sensor. The average skin temperature is calculated based on measurements from three body-placed sensors, namely, scapula, chest and arm (Figure 2). The skin temperature measurements are performed using one Shimmer (Shimmer-Sensing, Dublin, Ireland) temperature sensor and two gSKIN® bodyTEMP patches (greenTEG, Zurich, Switzerland). Two heat flux gSKIN® patches are

placed on both the chest and the left arm (Figure 2). The skin temperatures and heat flux measurements are acquired at a sampling frequency of 1 Hz. All the measured from the wearable sensors were received and saved on a smart phone. Core body temperature is estimated based on aural temperature measure measurements, which is performed using in-ear wireless (Bluetooth) temperature sensor (Cosinuss One, Düsseldorf, Germany) with a sampling rate if 1 Hz. At the end of each applied temperature level during the course of both experimental phases, a thermal sensation questionnaire, based on ASHRAE seven-point thermal scale, is performed for each test subject.

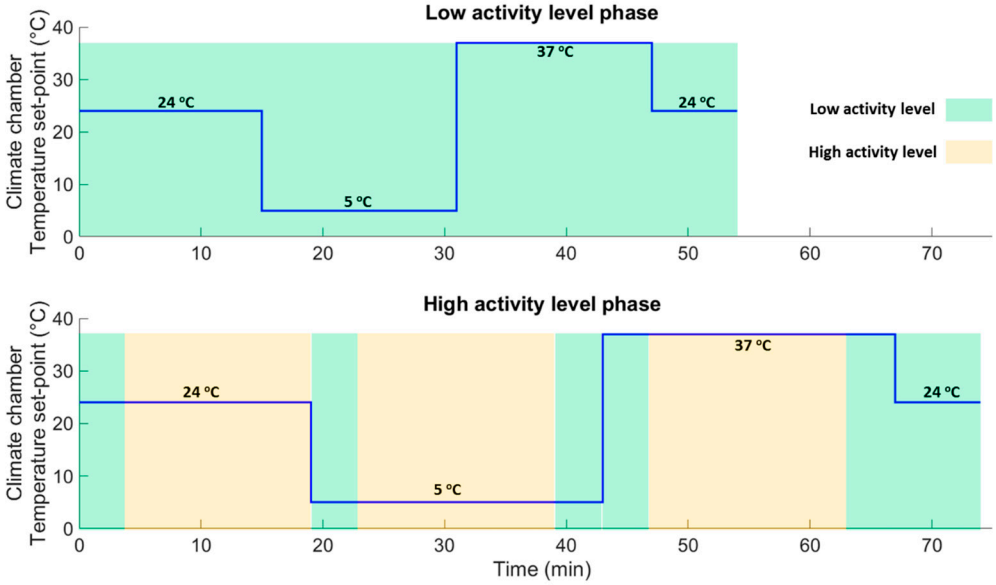

Figure 1. Plots showing the climate chambers' set-point temperatures programed during the 55 min low activity phase (upper graph) and the 75 min high activity phase (lower graph).

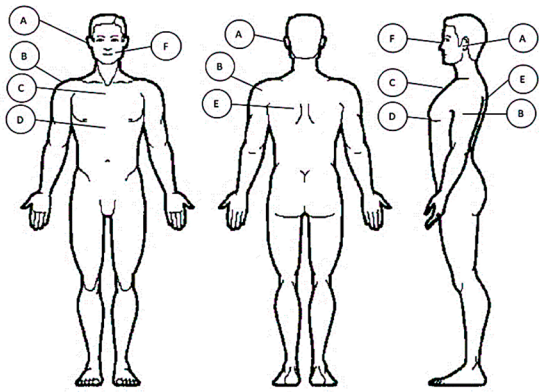

Figure 2. Sensor placement. (**A**) Ear channel for aural temperature measurement via the Cosinuss One; (**B**) upper arm where the skin temperature and heat flux are measured with the gSKIN patch; (**C**) middle upper chest where the skin temperature and heat flux are measured with the gSKIN patch; (**D**) lower chest where the heart rate is measured with the Polar H7; (**E**) scapula where skin temperature is measured with the Shimmer sensor; (**F**) mouth and nose where metabolic rate is measured via a MetaMAX-3B spiroergometer sensor.

2.2. Modelling and Classification

For the sake of present study, the measured variables are divided into wearables, which are easily measured variables using wearable sensors and gold standards (reference) variables, which are not suitable for wearable technologies. The wearables include heart rate H_R, aural temperature T_{er}, average skin temperature $\overline{T}_{sk}$, skin heat flux q_{sk} and ambient air temperature T_{∞}. On the other hand, the gold

standards consist of the core temperature T_c, which is driven from the aural temperature [$T_c = f(T_{er})$], metabolic rate M_r and personal thermal sensation votes TS. The ultimate goal of this work is to develop an adaptive classification model to predict the individual thermal sensation depending, solely, on the wearables or estimated variables. Hence, both of the metabolic rate and core body temperature are estimated using an online dynamic modelling approach (Figure 3). Then, the individual thermal sensation is predicted using a classification model (classifier) whose inputs are the wearables and estimated the metabolic rate and core body temperature (Figure 3).

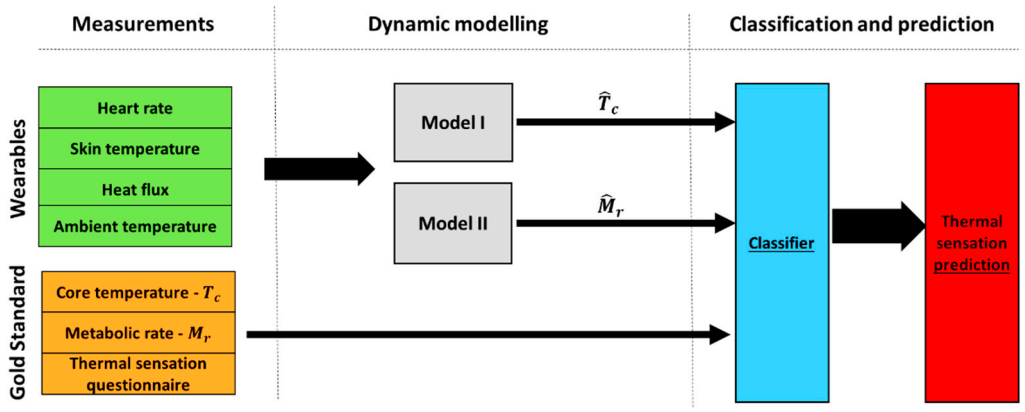

Figure 3. Overview of the main steps to predict the individual thermal sensation.

2.2.1. Dynamic Modelling

Although the system under study (occupant's thermoregulation) is inherently a non-linear system, the essential perturbation behaviour can often be approximated well by simple linearized transfer function (TF) models [17–19]. For the purposes of the present paper, therefore, the following linear, multi-input, single-output (MISO) discrete time systems are considered to estimate metabolic rate and core body temperature [18]:

$$y(k) = \sum_{r=1}^{r=R} \frac{B_r\left(z^{-1}\right)}{A_r(z^{-1})} u_r(k-\delta_r) + \xi(k), \tag{1}$$

where k denotes the value of the associated variable at the kth sampling instant; $y(k)$ is the output variable; $u_r(k)$, $r = 1, 2, \ldots, R$ are input variables, while $A\left(z^{-1}\right)$ and $B\left(z^{-1}\right)$ are appropriately defined polynomials in the backshift operator z^{-1}, i.e., $z^{-i}y(k) = y(k-i)$ and $\xi(k)$ is additive noise, a serially uncorrelated sequence of random variables with variance σ^2 that accounts for measurement noise. The simplified refined instrumental variable (SRIV) algorithm was utilised in the identification and estimation of the models (model parameters and model structure) [20]. Two main statistical measures were employed to determine the most appropriate model structure. Namely, the coefficient of determination R_2^T, based on the response error; and YIC (Young's information criterion), which provides a combined measure of model fit and parametric efficiency, with large negative values indicating a model which explains the output data well and yet avoids over-parameterisation [21]. Additionally, the estimation performance of the selected models is evaluated used the mean absolute error (MAE) value.

2.2.2. Classification Model

To predict the individual thermal sensation, a classification model (classifier) is developed and trained based on the wearables and estimated variables (metabolic rate and core body temperature), together with the thermal sensation votes (gold standard). A modified support vector machine (SVM) technique, namely, the least squares support vector machine (LS-SVM), is used to develop and train the thermal sensation classifier [22,23]. SVMs are originally presented as binary classifiers [22] that assign each data instance $X \in \mathbb{R}^d$ to one of two classes described by a class label $y \in \{-1, 1\}$ based on

the decision boundary that maximises the margin $2/\|\mathbf{w}\|_2$ between the two classes. Generally, a feature map $\varphi: \mathbb{R}^d \Rightarrow \mathbb{R}^p$ is used to transform the geometric boundary between the two classes to a linear boundary $L: \mathbf{w}^T\varphi(x) + b = 0$ in feature space, for some weight vector $\mathbf{w} \in \mathbb{R}^{p\times 1}$ *and* $b \in \mathbb{R}$. The class of each instance can then be found by $y = sign\left(\mathbf{w}^T\varphi(x) + b\right)$, where *sign* refers to the sign function. Due to some computational complexities of standard SVM because of the quadratic programming problem, the least squares support vector machine (LS-SVM) is presented to overcome such problem. LS-SVM, in contrast with standard SVM, relies on a least squares cost function as follows:

$$\min_{\mathrm{w,\ b;}\ e} \frac{1}{2}\mathbf{w}^T\mathbf{w} + \gamma\sum_{\mathrm{i}=1}^{N} e_i^2, \tag{2}$$

such that $y_i\left(\mathbf{w}^T\varphi(x_i) + b\right) \geq 1 - e_i$ *and* $e_i \geq 0,\ i = 1,\ 2,\ \ldots,\ N$, where e_i errors such that $1 - e_i$ is proportional to the signed distance of x_i from the decision boundary, and γ represents the regularisation constant. In LS-SVM, instead of solving the quadratic programming problem, a set of linear equations to be solved is sufficient to find the optimal solution of the classifier. The LS-SVMlab (Least Squares Support Vector Machine lab) Matlab-based toolbox is used to implement the LS-SVM classification algorithm [22].

The performance of the classification model is determined based on accuracy, sensitivity, precision and F1-score as follows:

$$Accuracy = \frac{TP + TN}{TP + TN + FP + FN},\ Sensitivity = \frac{TP}{TP + FN}$$

$$Precision = \frac{TP}{TP + FP},\ F1Score = \frac{2 * Precision * Sensitivity}{Precision + Sensitivty}$$

where *TP*, *TN*, *FP* and *FN* are the true positive, true negative, false positive and false negative, respectively.

3. Results and Discussion

3.1. Dynamic Modelling and Estimation of an Individual's Metabolic Rate

The average metabolic rate obtained from the 25 participants at the temperature levels (24, 5 and 37 °C) during low and high activity phases are presented in Table 2.

Table 2. Average (±standard deviation) of the measured metabolic rate obtained from the 25 test subjects during low and high activity phases.

	Measured Metabolic Rate (MET *)	
Temperature	**Low Activity Phase**	**High Activity Phase**
24 °C	1.19 ± 0.19	5.11 ± 1.18
5 °C	1.18 ± 0.23	5.32 ± 1.24
37 °C	1.22 ± 0.17	5.48 ± 1.20

* 1MET = 1.163 W·kg^{-1}.

Different combinations of input variables (wearables) are tested for the best estimation of an individual's metabolic rate. The SRIV algorithm, combined with *YIC* and R_2^T selection criteria, suggested that a second-order MISO discrete-time TF with heart rate (H_R), average skin heat flux ($\overline{q}_{sk}$) and aural temperature (T_{er}) as input variables is the best (with average R_2^T = 0.89 ± 0.04 and *YIC* = −13.62 ± 2.33) to describe and estimate the dynamic behaviour of the individual's metabolic rate. More specifically, the SRIV algorithm identified the following general MISO discrete-time TF model structure:

$$\hat{M}_r(k) = \left[\frac{B_1\left(z^{-1}\right)}{A(z^{-1})}\frac{B_2\left(z^{-1}\right)}{A(z^{-1})}\frac{B_3\left(z^{-1}\right)}{A(z^{-1})}\right].\begin{bmatrix} T_{er}(k-\delta_1) \\ H_R(k-\delta_2) \\ \overline{q}_{sk}(k-\delta_3) \end{bmatrix} + \xi(k) \quad (3)$$

where $\hat{M}_r(k)$ is the estimated metabolic rate and the numerator polynomials B_1, B_2 and B_3 are of the following orders (number of zeros) 2, 3 and 2, respectively. The system delays δ_1, δ_2 and δ_3 are varied from person to another (inter-personal) with average values of 1.4, 0.20 and 0.21 min, respectively (Table 3). A simulation example of the developed estimation model (Equation (3)) for one test subject during the low activity experimental phase at normal temperature (24 °C) is depicted in Figure 4.

Table 3. Average R_2^T, *YIC*, model delays and MAPE for the selected MISO-DTF model to estimate the individual's metabolic rate obtained from the 25 test subjects during low and high activity phases.

	Average R_2^T ± std	Average *YIC* ± std	Model Delays Average [δ_1 δ_2 δ_3]	Average *MAPE* ± std
Low activity phase	0.85 ± 0.02	−12.32 ± 3.4	[1.5 0.3 0.25] min	10 ± 2.2%
High activity phase	0.94 ± 0.03	−14.43 ± 2.8	[1.2 0.18 0.20] min	7.6 ± 2.6%

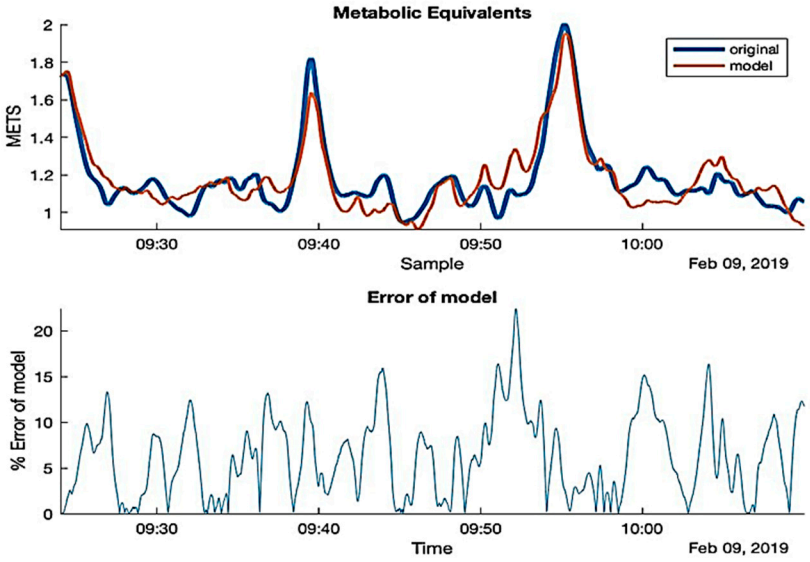

Figure 4. A simulation example of the developed MISO-DTF model (Equation (3)) to estimate the metabolic rate during the low activity experimental phase at normal temperature (24 °C).

The estimation performance of the selected general MISO-DTF (Equation (3)) is evaluated based on the mean absolute percentage error ($MAPE = \frac{100\%}{N}\sum_{k=1}^{N}\left|\frac{\hat{M}_r(k)-M_r(k)}{M_r(k)}\right|$) value.

The results have shown that the developed general model (Table 3), for all test subjects, a higher average MAPE value (10 ± 2.2%) during the low activity phases than the average MAPE value (7.6 ± 2.6%) resulted during the high activity phases. The METs (metabolic equivalent tasks) are a measure which accounts for a normalized form of energy expenditure per kilogram of mass. There is a consensus that the measurement of the metabolic rate might vary among individuals (interpersonal) up to 75% [24], even within the same day from morning to afternoon for the same subject (intrapersonal) up to 6%, though measurements on different days might be comparable on fasted subjects [25]. Hence, a general estimation model of individual metabolic rate will not be efficient in this case. However, the general estimation performance of the suggested general MISO model can be enhanced by using the online adaptive form of the SRIV algorithm [26]. The online adaptive (closed-loop) SRIV algorithm provides the possibility to personalise the developed general model by retuning the model parameters and model delays based on the streaming data acquired from the wearable sensors.

3.2. Classification Model and Prediction of Individual's Thermal Sensation

In order to give an idea about the interaction relationship between considered variables, the correlation between all measured variables are calculated and represented in a colour-map Pearson correlation coefficient (r) matrix, as shown in Figure 5. High positive or negative correlation coefficient values, such as that between heat flux and skin temperature, are reflected as a strong interaction between these variables, which can affect the feature selection of the classification model.

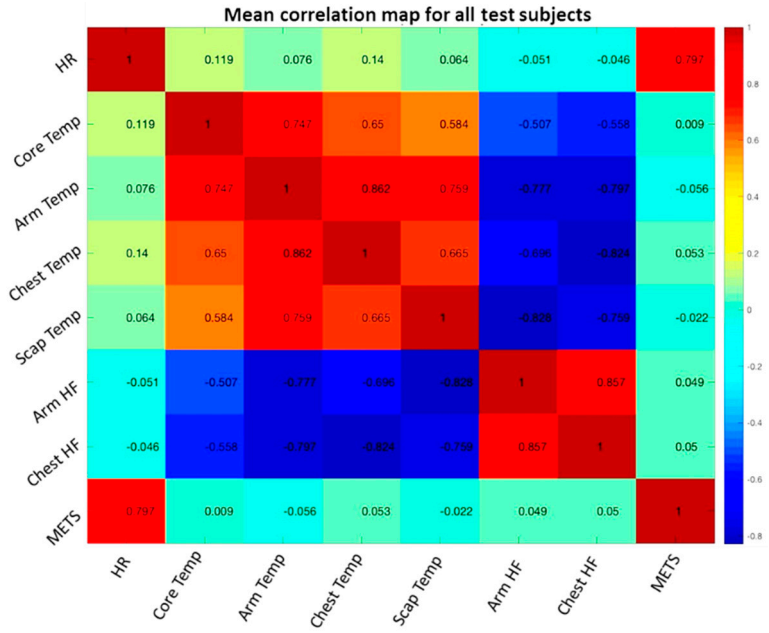

Figure 5. Colour-map of the correlation matrix representing the correlation levels ($r \in [-1, 1]$) between the mean values of all measured variables, namely, heart rate (HR), aural (core) temperature, arm temperature, chest temperature, scapula temperature, heat flux from the arm skin (Arm HF), heat flux from the chest skin (Chest HF) and metabolic rate (METs).

The classification model for predicting the individual's thermal sensation is developed, based on the LS-SVM approach, by training the classifier on 80% of the data points, while the rest of the data (20%) is used for testing. The model accuracy, sensitivity F1-score and overall confusion matrix are computed to evaluate the performance of the developed classifier. The feature space includes all the measured and estimated input variables, namely, T_{er}, H_R, $\overline{q}_{sk}$, $\overline{T}_{sk}$, $\Delta\overline{T} = T_{er} - \overline{T}_{sk}$ and $\hat{M}_r$. Additionally, other features are extracted by computing the variance, min, max, root mean squares (RMS) and first derivative ($\frac{dx}{dt}$, where x is the variable) of the aforementioned measured and estimated variables. The age and gender of the test subjects are also included in the feature spaces.

Figure 6 is showing the distribution of the participants' thermal sensation votes at the three environment temperatures (24, 5 and 37 °C). The aforementioned figure shows the 'confusion space', or the area in which the reported thermal sensation votes at the three environmental temperatures are overlapping. Such observation shows that the thermal perception may overlap even with large differences in the surrounding environmental temperatures. Such a confusion space is a great challenge for any predictive model of thermal sensation, especially for static models such as PMV.

For the sake of the main objective of the present work, the computational cost of the developed algorithm should be low enough to be compatible with wearable technology and online modelling. Hence, a feature selection procedure is employed to obtain the most reduced-dimension model yet with the best error performance. Feature selection here is based on evaluating all possible feature combinations and selecting the combination with best error performance. The feature selection step results in a feature space including 25 features, as shown in Table 4.

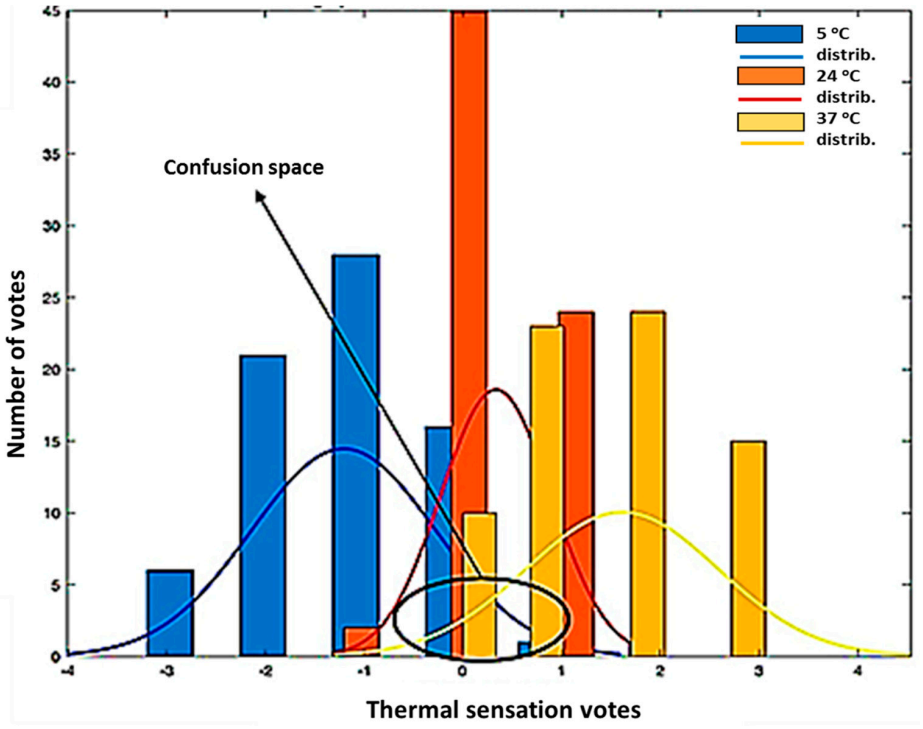

Figure 6. Distribution (distrib.) of the participants' (25) thermal sensation votes at the three environment temperatures (24, 5 and 37 °C) showing the confusion space.

Table 4. An overview of the selected feature space including the measured and estimated variables (six variables) and some operations on these variables (× = selected).

	Variance	Min	Max	RMS	$\frac{d}{dt}$
T_{er}	×	×	×	×	-
H_R	×	×	×	×	-
$\overline{q}_{sk}$	×	×	×	×	×
$\overline{T}_{sk}$	×	-	-	×	-
$\Delta\overline{T}$	×	×	×	×	-
$\hat{M}_r$	-	-	-	-	-

A classification model is developed based on the selected 25 input features and trained using the LS-SVM approach. The resulting confusion matrix from the developed classification model based on the selected feature space is shown in Figure 7.

The overall error performance results of the developed classification model are presented in Table 5. For a seven-class classification problem, the developed classifier have shown an overall accuracy of 76% to predict the individual's thermal sensation. The developed classifier has shown a high (84%) F1-score, which reflects low false-positives and -negatives.

Table 5. Overall error performance (accuracy, sensitivity, precision and F1-score) of the developed general LS-SVM classification model.

Measure	Value
Accuracy	0.76
Sensitivity	0.82
Precision	0.87
F1 score	0.84

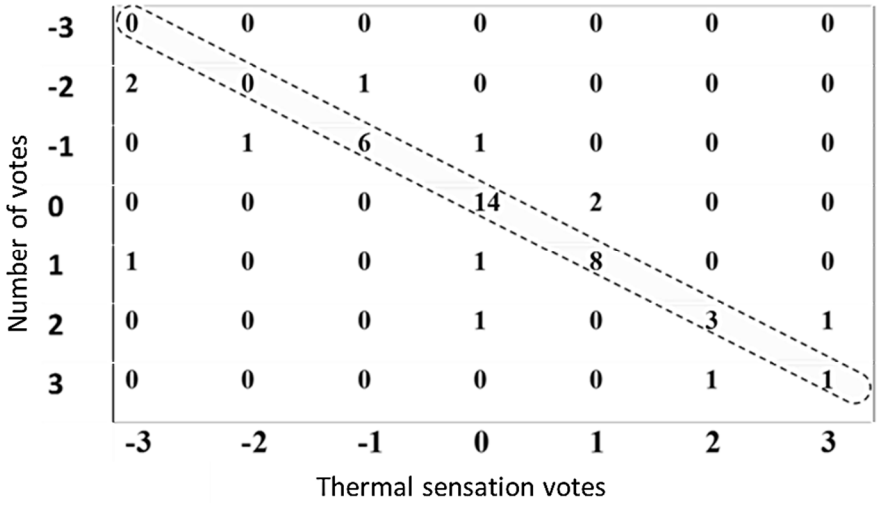

Figure 7. The resulted confusion matrix from testing the developed LS-SVM classifier. The diagonal represents the correctly-classified data points.

The error performance results of the developed general classification for each class separately are shown in Table 6. The results showed that the error performances of classes 1, 2, 6 and 7 are very low (see Table 6), which can be attributed to the low number (0, 2, 4 and 2, respectively) of obtained votes for these classes, or, in other words, due to the uneven class distribution. Therefore, the overall F1-score is a more reliable and efficient measure of performance than the accuracy in this case.

Table 6. The error performance (precision, sensitivity and F1-score) of the developed general LS-SVM model for the seven-class classification problem.

	Class 1	Class 2	Class 3	Class 4	Class 5	Class 6	Class 7
Sensitivty	-	0	0.75	0.88	0.80	0.60	0.50
Precision	0	0	0.86	0.82	0.80	0.75	0.50
F1-score	0	0	0.80	0.85	0.80	0.67	0.50

SVM is used in recent studies to assess the occupant's thermal demands [12] and to predict thermal comfort/sensation [11]. In these studies, the results have shown that SVM is able to predict thermal comfort/sensation with accuracy and F1 scores of 76.7% and 84%, respectively. However, these results is only obtained by reducing the seven-class classification problem to a three-class problem. Hence, we believe that reducing the number of classes will improve our suggested general model performance. Moreover, based on streaming data obtained from wearable sensor technologies, a personalised adaptive classification model, based on the same extracted features, will enhance the model performance to predict the individual's thermal sensation. Different related works investigated the problem of thermal sensation and comfort prediction via machine learning algorithms. Ghahramani et al. [27] applied the hidden Markov model (HMM) technique to the thermal comfort prediction problem with three levels of thermal comfort. The main issue in the used dataset in this study is the class imbalance, which is not tackled by the proposed methodology. A recent study by Lu et al. [7] proposed a personalised model, however, the study strictly investigated two subjects and developed a dedicated model for each subject.

Testing of the trained model for each test subject was implemented using the Matlab platform on a computer with Intel® 8 Core i7 (2.7 GHz) processor and 16 GB of RAM. The average computational time for one test run on this computer was 100 ms. The developed model should be trained using data from different populations (e.g., different ages, ethnicities and physical conditions) and different environmental conditions (e.g., broader ranges of temperature and humidity). In future research, the mental status of the participants should be taken into the account to investigate the capability of the

developed model to comply with different mental conditions (e.g., stresses). Moreover, a sensitivity analysis should be performed considering different accuracy and sensitivity levels of the wearable sensors. On the other hand, the LS-SVM approach used in this paper is suitable for online adaptation with a flexibility to receive new data (streaming data) variables. Hence, the developed model can be used for adaptive real-time mode-based monitoring of individual thermal sensation. Additionally, as such, the developed mode is suitable for different applications such as the simulation of the human thermal state under different environmental conditions and for building design and control. In this paper, we present the possibility of using this model for adaptive HVAC control systems.

3.3. Adaptive Occupant-Based HVAC Predictive Controller

In modern buildings, it is very common that HVAC control systems are designed in such way to ensure parsimonious energy use and cost-effective building operation. This often happens by tuning HVAC control parameters (e.g., set points) to exploit the inherent trade-off between energy consumption and thermal comfort, with the latter acting as a constraint defining a theoretical and practical upper bound on potential energy savings [28–30]. In this paper, we suggested a model-predictive control (MPC) strategy, which is based on continuous feedback of occupant's thermal state (sensation/comfort) with main control objective to achieve occupant's thermal comfort. Then the energy use can be employed in the controller's cost-function as constraints.

In this section, we introduced to an adaptive occupant-based HVAC predictive controller using the developed LS-SVM predictive classification model. The general framework of the proposed HVAC predictive controller approach is depicted in Figure 8. In this paper, we only describe the main methodology to use the LS-SVM predictive classification model for the occupant's thermal state in the generalized predictive control (GPC) scheme, which will be studied and investigated further in future work. The GPC is one of the most popular model predictive controlling (MPC) methods in broad number of fields. The basic principle of GPC is to calculate a sequence (control horizon, N_c) of future control signals that minimizes a cost function defined over a prediction horizon (N_p) [31]. In general, the GPC algorithm consists of two main subsystems, namely, a prediction model and an optimizer. As shown in Figure 8, two main components, namely, the adaptive algorithm for LS-SVM predictive model and the GPC algorithm, are suggested.

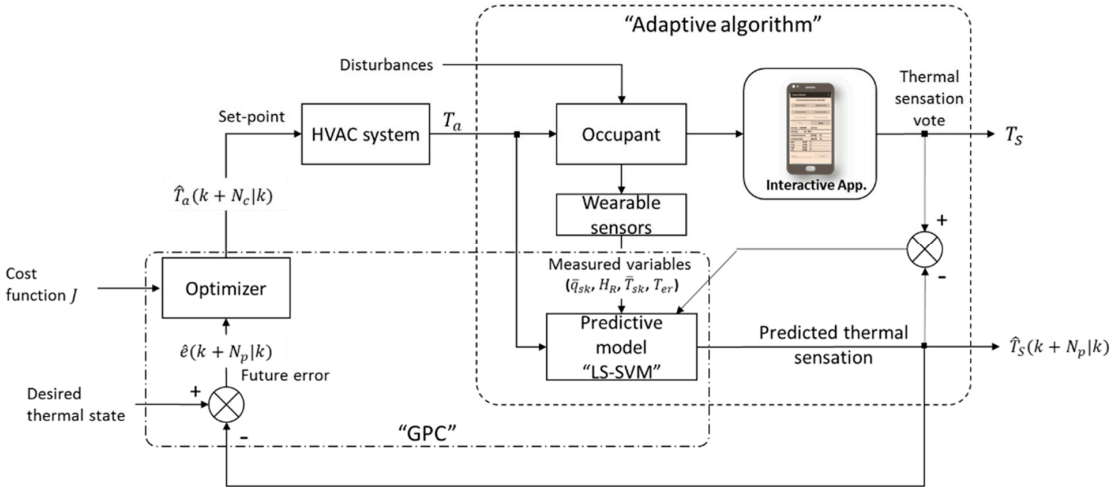

Figure 8. Block diagram of the proposed adaptive HVAC LS-SVM-based model predictive controller.

3.3.1. Adaptive LS-SVM-Based Algorithm for Predicting the Occupant's Thermal Sensation

The availability of the real-time sensors data, from the wearable technologies, has given the possibility of streaming data, which are processed via the proposed online streaming algorithm to adapt the classifier model. This adaptive algorithm is needed to handle the newly arrived data (streaming

data) in the training set. Different approaches are available in the literature to handle these challenges, such as incremental learning methods [32], which work on adapting and retuning the parameters of the general model based on the newly collected data. Another approach is the localized learning, which is based on developing a local model for each test point or subset of the test set [33]. The streaming data includes:

i. Wearable sensor data, which consists of the continuously (easily) measured variables, namely, occupant's heart rate, skin heat flux, skin temperature, ambient temperature and aural temperature.
ii. Data obtained from the interactive mobile application, which consists of the occupant's data, namely, age and gender. Additionally, the occupant's thermal sensation vote (T_S) is to be obtained via mobile application-based questioner (interactive application).

3.3.2. The GPC Algorithm

In general, the goal of any controller is to calculate the input (control signal) to the controlled system (plant) such that the output follows the desired reference. However, in case of the predictive controller, the GPC algorithm aims to find the best-predicted output sequence (using the prediction model) that is the closest to a predefined reference trajectory (desired thermal state in our case). The *prediction model* in our case is the adaptive LS-SVM classification model that predicts the occupant's thermal sensation (T_S). The algorithm simulates multiple future scenarios (predicted output sequence) in a systematic way using the *optimizer*, then the predicted output $\hat{T}_S(k+N_p|k)$ is used to calculate the optimal future input (ambient temperature, $\hat{T}_a(k+N_c|k)$). The optimizer solves an online optimization problem based on a defined *cost function* (Figure 8), which minimizes the predicted error $\hat{e}(k+N_p|k)$ between the reference $R_S(k)$ and the predicted output $\hat{T}_S(k+N_p|k)$. The cost-function is given as follows [34]:

$$J\left(N_1, N_p, N_c\right) = \sum_{j=N_1}^{N_p} \alpha_j \left[\hat{T}_S(k+j\,|\,k) - R_S(k+j)\right]^2 + \sum_{j=1}^{N_c} \lambda_j [\Delta T_a(k+j-1)]^2 \quad (4)$$

where $\Delta T_a(k)$ is the change in the control signal (ambient temperature), $\hat{T}_S(k+j\,|\,k)$ is the predicted output (thermal sensation) sequence, $R_S(k)$ is the reference (desired level of thermal sensation), N_1 is the minimum of the prediction horizon and α and λ are the weighting factors. The suggested control signal ($\hat{T}_a$) can be incorporated into the HVAC system by feeding it as a set-point to the HVAC controller. The sequence of predicted thermal sensation is crucial in the optimisation (cost function) of the control (manipulated) variables [35,36]. In the presented approach, we have considered the air temperature as the only manipulated variable; however, more HVAC-related variables can be added to the optimisation step (e.g., ventilation rate and energy consumption).

The proposed approach (Figure 8) depends on the extracted features from easily measured variables (T_{er}, H_R, $\overline{q}_{sk}$ and $\overline{T}_{sk}$,) that can be collected from already available (off-the-shelf) wearable sensors (e.g., smart watches and on-body smart tags). As such, this proposed approach has the advantage over other models (e.g., [37]), which depend on difficult and/or invasive measurements (core body temperature and metabolic rate) and, consequently, not convenient for long-term monitoring. Moreover, the used LS-SVM used in this approach is suitable for online prediction of an individual's thermal state with minimum computational cost (100 ms for the prediction of the thermal sensation of each individual).

4. Conclusions

In this present paper, 25 participants are subjected to three different environmental temperatures, namely 5 °C (cold), 20 °C (moderate) and 37 °C (hot), at two different activity levels, namely, at low level (rest) and high level (cycling at 80 W power). Metabolic rate, heart rate, average skin temperature

(from three different body locations), heat flux and aural temperature are measured continuously during the course of the experiments. The thermal sensation votes are collected from each test subject based on the ASHRAE seven-point questionnaire. The results have shown that a reduced-ordered (second-order) MISO-DTF including three input variables (wearables), namely, aural temperature, heart rate and average heat flux, is best to estimate the individual's metabolic rate (non-wearable) with an average MAPE of 8.7%. A general classification model based on the LS-SVM technique is developed to predict the individual's thermal sensation. For a seven-class classification problem, the results have shown that the overall model accuracy and F1-score of the developed classifier are 76% and 84%, respectively. It is suggested in this paper that the overall performance of the model can be enhanced by using a personalised adaptive classification algorithm based on streaming data from wearable sensors. The developed LS-SVM classification model for the prediction of the occupant's thermal sensation can be integrated in the HVAC system to provide an occupant thermal state-based climate controller. In this paper, we introduced an adaptive occupant-based HVAC predictive controller using the developed LS-SVM predictive classification model.

Author Contributions: Conceptualisation: A.Y. and J.-M.A.; methodology: A.Y. and N.C.; software: A.Y.; validation: A.Y.; formal analysis: A.Y. and N.C.; investigation: A.Y. and N.C.; resources: J.-M.A.; data curation: A.Y. and N.C.; writing—original draft preparation: A.Y. and N.C.; writing—review and editing: A.Y. and J.-M.A.; visualisation: A.Y.; supervision: J.-M.A. and A.Y.; project administration: J.-M.A.; funding acquisition: J.-M.A.

Funding: This research received no external funding.

Conflicts of Interest: The authors declare no conflict of interest.

References

1. ASHRAE. *Thermal Environmental Conditions for Human Occupancy*; American Society of Heating, Refrigeration and Air Conditioning Engineers, Inc.: Atlanta, GA, USA, 2004.
2. ISO-10551. *Ergonomics of the Thermal Environment—Assessment of the Influence of the Thermal Environment Using Subjective Judgement Scales*; ISO: Brussels, Belgium, 1995.
3. Koelblen, B.; Psikuta, A.; Bogdan, A.; Annaheim, S.; Rossi, R.M. Thermal sensation models: A systematic comparison. *Indoor Air* **2017**, *27*, 680–689. [CrossRef] [PubMed]
4. Enescu, D. Models and Indicators to Assess Thermal Sensation Under Steady-State and Transient Conditions. *Energies* **2019**, *12*, 841. [CrossRef]
5. Kenneth, C. *Parsons, Human Thermal Environments: The Effects of Hot, Moderate, and Cold Environments on Human Health, Comfort, and Performance*, 3rd ed.; CRC Press: Boca Raton, FL, USA, 2014.
6. Nikolopoulou, M.; Steemers, K. Thermal comfort and psychological adaptation as a guide for designing urban spaces. *Energy Build.* **2003**, *35*, 95–101. [CrossRef]
7. Lu, S.; Wang, W.; Wang, S.; Hameen, E.C. Thermal Comfort-Based Personalized Models with Non-Intrusive Sensing Technique in Office Buildings. *Appl. Sci.* **2019**, *9*, 1768. [CrossRef]
8. De Dear, R.; Brager, G.S. Developing an adaptive model of thermal comfort and preference. *ASHRAE Trans.* **1998**, *104*, 145–167.
9. Kim, J.; Zhou, Y.; Schiavon, S.; Raftery, P.; Brager, G. Personal comfort models: Predicting individuals' thermal preference using occupant heating and cooling behavior and machine learning. *Build. Environ.* **2018**, *129*, 96–106. [CrossRef]
10. Chaudhuri, T.; Soh, Y.C.; Li, H.; Xie, L. Machine learning based prediction of thermal comfort in buildings of equatorial Singapore. In Proceedings of the 2017 IEEE International Conference on Smart Grid and Smart Cities (ICSGSC), Singapore, 23–26 July 2017; pp. 72–77.
11. Farhan, A.A.; Pattipati, K.; Wang, B.; Luh, P. Predicting individual thermal comfort using machine learning algorithms. In Proceedings of the 2015 IEEE International Conference on Automation Science and Engineering (CASE), Gothenburg, Sweden, 24–28 August 2015; pp. 708–713.
12. Dai, C.; Zhang, H.; Arens, E.; Lian, Z. Machine learning approaches to predict thermal demands using skin temperatures: Steady-state conditions. *Build. Environ.* **2017**, *114*, 1–10. [CrossRef]

13. Huang, C.-C.J.; Yang, R.; Newman, M.W. The potential and challenges of inferring thermal comfort at home using commodity sensors. In Proceedings of the 2015 ACM International Joint Conference on Pervasive and Ubiquitous Computing-UbiComp'15, Osaka, Japan, 7–11 September 2015; pp. 1089–1100.
14. Hussain, S.; Kang, B.H.; Lee, S. *A Wearable Device-Based Personalized Big Data Analysis Model*; Information Technology in Bio- and Medical Informatics; Springer: Cham, Switzerland, 2014; Volume 8867, pp. 236–242.
15. ASHRAE. *ASHRAE Standard 55. Atlanta GA: American Society of Heating*; Refrigerating and Air-Conditioning Engineers, Inc.: Atlanta, GA, USA, 2017.
16. Dewhirst, M.W.; Viglianti, B.L.; Lora-Michiels, M.; Hanson, M.; Hoopes, P.J. Basic principles of thermal dosimetry and thermal thresholds for tissue damage from hyperthermia. *Int. J. Hyperth.* **2003**, *19*, 267–294. [CrossRef]
17. Young, P.C. *Control and Dynamic Systems: Advances in Theory and Applications*; Academic Press Inc., Elsevier Science: New York, NY, USA, 1989.
18. Young, P.C. *Concise Encyclopedia of Environmental Systems*, 1st ed.; Pergamon-Elsevier Science Ltd.: Oxford, UK, 1993.
19. Youssef, A.; D'Haene, M.; Vleugels, J.; De Bruyne, G.; Aerts, J.-M. Localised Model-Based Active Controlling of Blood Flow During Chemotherapy to Prevent Nail Toxicity and Onycholysis. *J. Med. Boil. Eng.* **2018**, *39*, 139–150. [CrossRef]
20. Young, P.; Jakeman, A. Refined instrumental variable methods of recursive time-series analysis Part III. Extensions. *Int. J. Control* **1980**, *31*, 741–764. [CrossRef]
21. Young, P.C.; Chotai, A.; Tych, W. *Identification, Estimation and Control of Continuous-Time Systems Described by Delta Operator Models*; Kluwer Academic Publishers: Dordrecht, The Netherlands, 1991.
22. Suykens, J.A.K.; Van Gestel, T.; De Brabanter, J.; De Moor, B.; Vandewalle, J. *Least Squares Support Vector Machines*; World Scientific Pub Co Pte Ltd.: Singapore, 2002.
23. Suykens, J.; Vandewalle, J. Least Squares Support Vector Machine Classifiers. *Neural Process. Lett.* **1999**, *9*, 293–300. [CrossRef]
24. Byrne, N.M.; Hills, A.P.; Hunter, G.R.; Weinsier, R.L.; Schutz, Y. Metabolic equivalent: One size does not fit all. *J. Appl. Physiol.* **2005**, *99*, 1112–1119. [CrossRef] [PubMed]
25. Haugen, H.A.; Melanson, E.L.; Tran, Z.V.; Kearney, J.T.; Hill, J.O. Variability of measured resting metabolic rate. *Am. J. Clin. Nutr.* **2003**, *78*, 1141–1144. [CrossRef] [PubMed]
26. Garnier, H.; Young, P.C.; Gilson, M. Simple Refined IV Methods of Closed-Loop System Identification. *IFAC Proc. Vol.* **2009**, *42*, 1151–1156. [CrossRef]
27. Ghahramani, A.; Castro, G.; Karvigh, S.A.; Becerik-Gerber, B. Towards unsupervised learning of thermal comfort using infrared thermography. *Appl. Energy* **2018**, *211*, 41–49. [CrossRef]
28. Kontes, G.D.; Giannakis, G.I.; Horn, P.; Steiger, S.; Rovas, D.V. Using Thermostats for Indoor Climate Control in Office Buildings: The Effect on Thermal Comfort. *Energies* **2017**, *10*, 1368. [CrossRef]
29. Ghahramani, A.; Zhang, K.; Dutta, K.; Yang, Z.; Becerik-Gerber, B. Energy savings from temperature setpoints and deadband: Quantifying the influence of building and system properties on savings. *Appl. Energy* **2016**, *165*, 930–942. [CrossRef]
30. Zavala, V.M. Real-Time Optimization Strategies for Building Systems. *Ind. Eng. Chem. Res.* **2013**, *52*, 3137–3150. [CrossRef]
31. Camacho, E.F.; Bordons, C. Model predictive control. *Int. J. Robust Nonlinear Control* **1999**, *13*, 280.
32. Losing, V.; Hammer, B.; Wersing, H. Incremental on-line learning: A review and comparison of state of the art algorithms. *Neurocomputing* **2018**, *275*, 1261–1274. [CrossRef]
33. Léon, B.; Vapnik, V. Local learning algorithms. *Neural Comput.* **1992**, *4*, 888–900.
34. Camacho, E.F.; Bordons, C. *Model Predictive Control*; Springer: London, UK, 2007.
35. Hosseini, S.M.; Carli, R.; Dotoli, M. Model Predictive Control for Real-Time Residential Energy Scheduling under Uncertainties. In Proceedings of the 2018 IEEE International Conference on Systems, Man, and Cybernetics (SMC), Miyazaki, Japan, 7–10 October 2018; pp. 1386–1391.

36. Afram, A.; Janabi-Sharifi, F. Theory and applications of HVAC control systems—A review of model predictive control (MPC). *Build. Environ.* **2014**, *72*, 343–355. [CrossRef]
37. Fiala, D.; Lomas, K.J.; Stohrer, M. Computer prediction of human thermoregulatory and temperature responses to a wide range of environmental conditions. *Int. J. Biometeorol.* **2001**, *45*, 143–159. [CrossRef] [PubMed]